High precision calculations of electroweak radiative corrections for polarized Møller scattering at one loop and beyond

Aleksandrs Aleksejevs
Memorial University, Grenfell Campus, Canada

Svetlana Barkanova
Acadia University, Canada

Yury Kolomensky
University of California, USA

Eduard Kuraev
JINR, Russia

Vladimir Zykunov
Belarusian State University of Transport, Belarus

Møller scattering at the tree level

The process of electron–electron scattering (Møller process)
C. Møller, Annalen der Physik 406, 531 (1932)

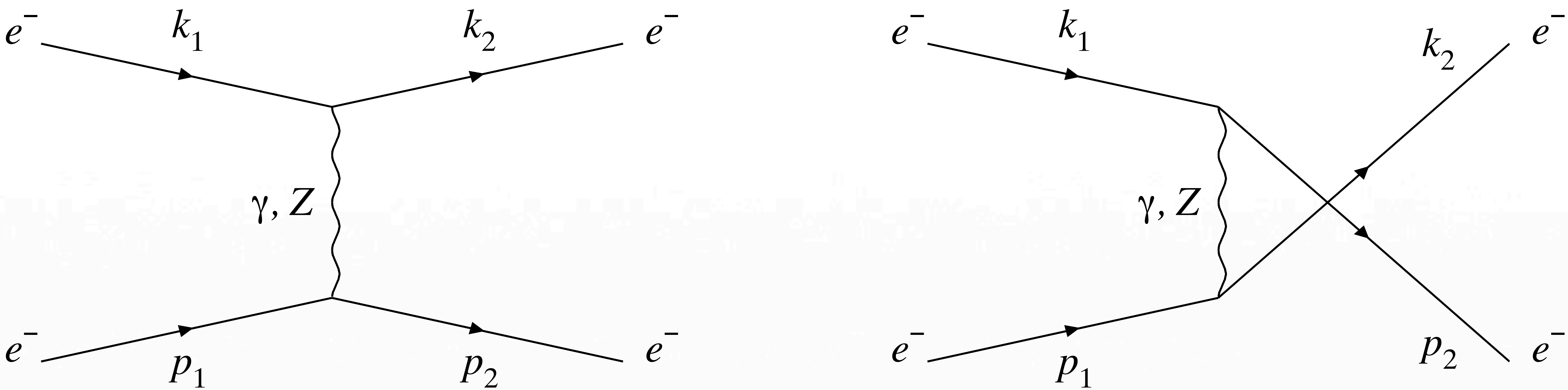

- Straightforward process!

$$A_{LR} = \frac{\sigma_{LL} + \sigma_{LR} - \sigma_{RL} - \sigma_{RR}}{\sigma_{LL} + \sigma_{LR} + \sigma_{RL} + \sigma_{RR}} = \frac{\sigma_{LL} - \sigma_{RR}}{\sigma_{LL} + 2\sigma_{LR} + \sigma_{RR}}$$

$$A^0_{LR} = \frac{s}{2m_W^2} \frac{y(1-y)}{1+y^4+(1-y)^4} \frac{\boxed{1-4s_W^2}}{s_W^2}, \quad y = -t/s$$

Motivation

The first observation of Parity Violation in Møller scattering was made by E-158 experiment at SLAC

$$Q^2 = 0.026 GeV^2, A_{LR} = (1.31 \pm 0.14(stat.) \pm 0.10(syst.)) \times 10^{-7}$$

$$\sin^2(\hat{\theta}_W) = 0.2403 \pm 0.0013 \text{ in } \overline{MS}$$

MOLLER, planned at JLab following the 11 GeV upgrade, will offer a new level of sensitivity and measure the parity-violating asymmetry in the scattering of longitudinally polarized electrons off unpolarized target to a precision of 0.73 ppb.

That would allow a determination of the weak mixing angle with an uncertainty of about 0.1%, a factor of five improvement in fractional precision over the measurement by E-158.

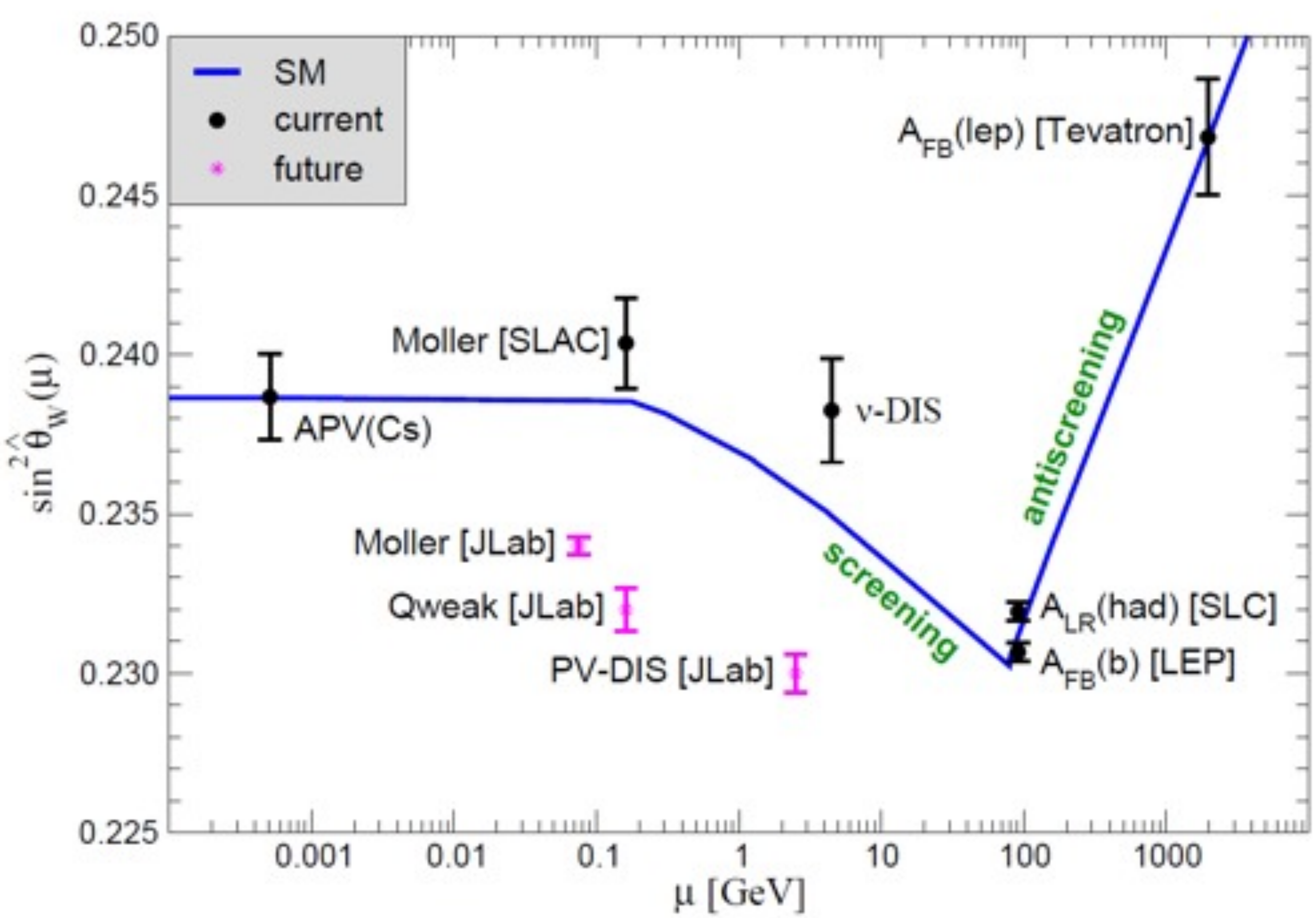

J. Benesch et al., MOLLER Proposal to PAC34, 2008

Motivation

Although PV asymmetry ($A_{LR} \sim 10^{-7}$) is very small, the accuracy of modern experiments exceeds the accuracy of the theoretical result in Born approximation. One–loop contribution was found to be rather big in the previous works:

A. Czarnecki, W. J. Marciano, Phys. Rev. D53, 1066 (1996);
A. Denner, S. Pozzorini, Eur. Phys. J. C7, 185 (1999);
A. Aleksejevs, S. Barkanova, A. Ilyichev, V. Zykunov, Phys. Rev. D82, 093013 (2010).

- Theoretical approach to control precision:
  - Make sure that everything is correct for the given level of perturbation (start with one loop)
    - For that we choose and compare two approaches: “by hand” and computer based using on-shell renormalization and using two different renormalization conditions (RC).
  - Determine if higher order effects (two-loops) are important
    - For that we compare results in two renormalization schemes (RS): on-shell and constrained differential renormalization (CDR). Size of the difference between RS will point out importance of higher order effects:
      W. Hollik and H.-J. Timme, Z. Phys. C. 33, 125 (1986).

One-loop

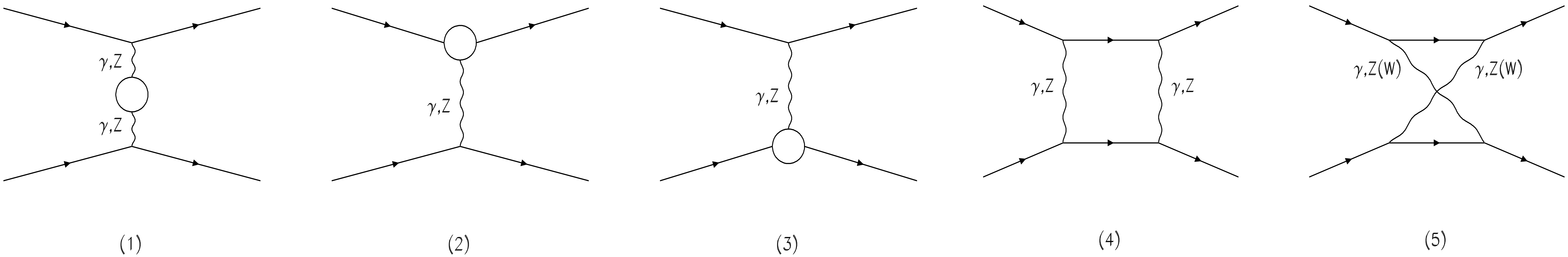

$$\sigma = \frac{\pi^3}{2s}|M_0 + M_1|^2 = \frac{\pi^3}{2s}(\underbrace{M_0 M_0^+}_{\propto\, \alpha^2} + \underbrace{2\mathrm{Re} M_1 M_0^+}_{\propto\, \alpha^3} + \underbrace{M_1 M_1^+}_{\propto\, \alpha^4}) = \sigma_0 + \sigma_1 + \sigma_Q$$

$$\sigma_1 = \sigma_1^{BSE} + \sigma_1^{Ver} + \sigma_1^{Box}$$

- Calculated in on-shell renormalization using:
  - Computer based using Feynarts, FormCalc, LoopTools and Form

    T. Hahn, Comput. Phys. Commun. 140 418 (2001);
    T. Hahn, M. Perez-Victoria, Comput. Phys. Commun. 118, 153 (1999);
    J. Vermaseren, (2000) [arXiv:math-ph/0010025]

  - "By hand" using approximations in small energy region $\frac{\{t,u\}}{m_{Z,W}^2} \ll 1$, for $\sqrt{s} \ll 30\ GeV$ and high energy approximation for $\sqrt{s} \gg 500\ GeV$

One-loop: renormalization conditions

- For a gauge invariant set, physical results should be invariant under different renormalization conditions.

- Renormalization constants are fixed by the renormalization conditions.
- Consider two classes:

1. The first determines the renormalization of the parameters and is related to physical observables at a given order of perturbation theory. These conditions are identical in both Hollik RC (HRC) and Denner RC (DRC).

$$\mathrm{Re}\hat{\Sigma}_T^W(m_W^2) = \mathrm{Re}\hat{\Sigma}_T^Z(m_Z^2) = \mathrm{Re}\hat{\Sigma}^f(m_f^2) = 0,$$

$$\hat{\Gamma}_\mu^{ee\gamma}\left(k^2 = 0,\, p^2 = m^2\right) = ie\gamma_\mu.$$

2. The second class fixes the renormalization of fields and is related to the Green's functions and has no effect on calculations of S-matrix elements.

$$\hat{\Sigma}_T^{\gamma Z}(0) = 0, \quad \frac{\partial}{\partial k^2}\hat{\Sigma}_T^{\gamma}(0) = 0$$

W. Hollik, Fortschr. Phys. 38, 165 (1990).

$$\hat{\Sigma}_T^{\gamma Z}(0) = 0, \quad \frac{\partial}{\partial k^2}\hat{\Sigma}_T^{\gamma}(0) = 0$$

$$\mathrm{Re}\hat{\Sigma}_T^{\gamma Z}(m_Z^2) = 0,\; \mathrm{Re}\frac{\partial}{\partial k^2}\hat{\Sigma}_T^Z(m_Z^2) = 0, \quad \mathrm{Re}\frac{\partial}{\partial k^2}\hat{\Sigma}_T^W(m_W^2) = 0.$$

A. Denner, Fortsch. Phys. 41, 307 (1993).

One-loop: renormalization conditions

Hollik RC (“by hand”)	Denner RC (computer based)
$\delta Z_\gamma^{(H)} = -\frac{\partial}{\partial k^2}\Sigma_T^\gamma(0)\,,$ $\delta Z_Z^{(H)} = \frac{\partial}{\partial k^2}\Sigma_T^\gamma(0) - 2\frac{c_W^2 - s_W^2}{s_W c_W}\frac{\Sigma_T^{\gamma Z}(0)}{m_Z^2}$ $+2\frac{c_W^2 - s_W^2}{s_W^2}\left(\frac{\delta m_Z^2}{m_Z^2} - \frac{\delta m_W^2}{m_W^2}\right),$ $\delta Z_W^{(H)} = \frac{\partial}{\partial k^2}\Sigma_T^\gamma(0) - 2\frac{c_W}{s_W}\frac{\Sigma_T^{\gamma Z}(0)}{m_Z^2}$ $+\frac{c_W^2}{s_W^2}\left(\frac{\delta m_Z^2}{m_Z^2} - \frac{\delta m_W^2}{m_W^2}\right),$ $\delta Z_{Z\gamma}^{(H)} = \frac{c_W s_W}{c_W^2 - s_W^2}\left(\delta Z_Z^{(H)} - \delta Z_\gamma^{(H)}\right).$	$\delta Z_W^{(D)} = -\mathrm{Re}\frac{\partial}{\partial k^2}\Sigma_T^W(m_W^2)\,,$ $\delta Z_Z^{(D)} = -\mathrm{Re}\frac{\partial}{\partial k^2}\Sigma_T^Z(m_Z^2)\,,$ $\delta Z_{Z\gamma}^{(D)} = \frac{2}{m_Z^2}\mathrm{Re}\Sigma_T^{\gamma Z}(0)\,,\ \delta Z_{\gamma Z}^{(D)} = -\frac{2}{m_Z^2}\mathrm{Re}\Sigma_T^{\gamma Z}(m_Z^2)\,,$ $\delta Z_\gamma^{(D)} = -\frac{\partial}{\partial k^2}\Sigma_T^\gamma(0)\,.$

W. Hollik, Fortschr. Phys. 38, 165 (1990).

A. Denner, Fortsch. Phys. 41, 307 (1993).

One-loop: renormalization conditions

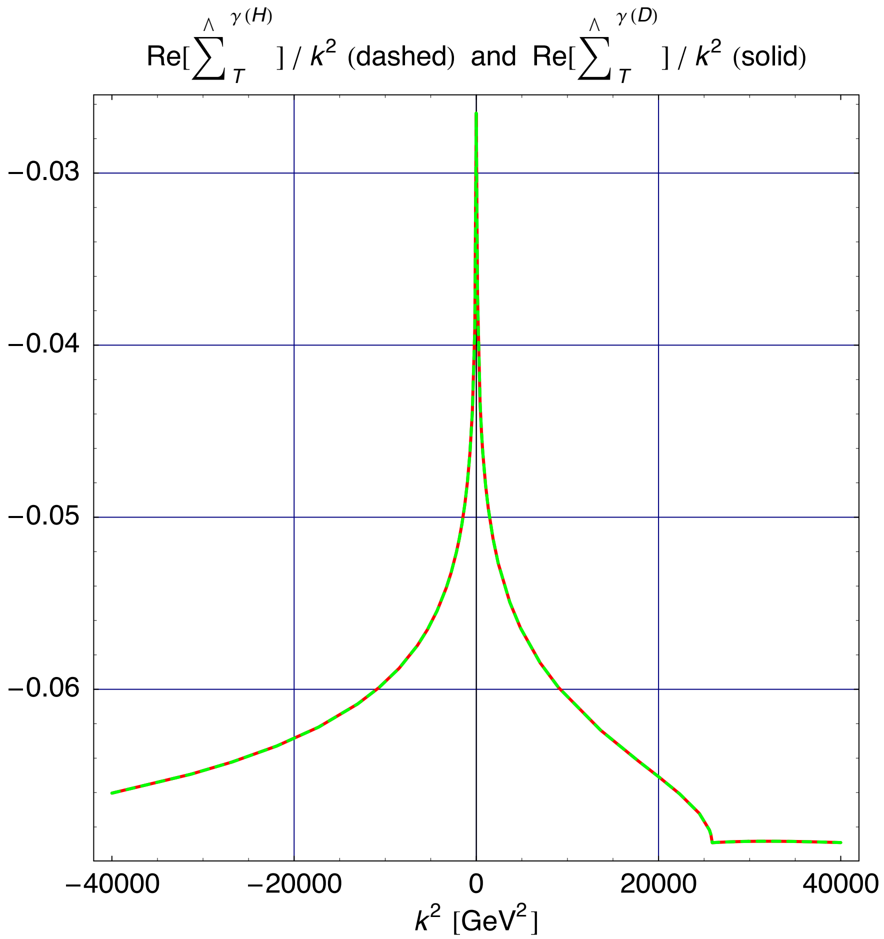

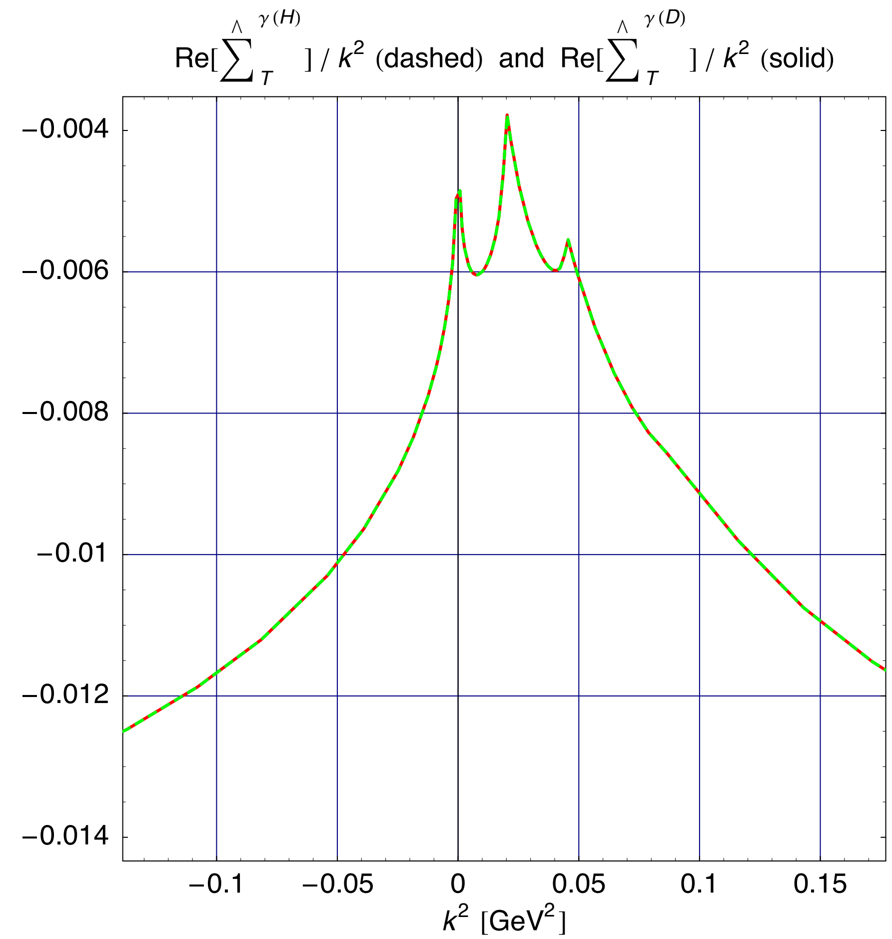

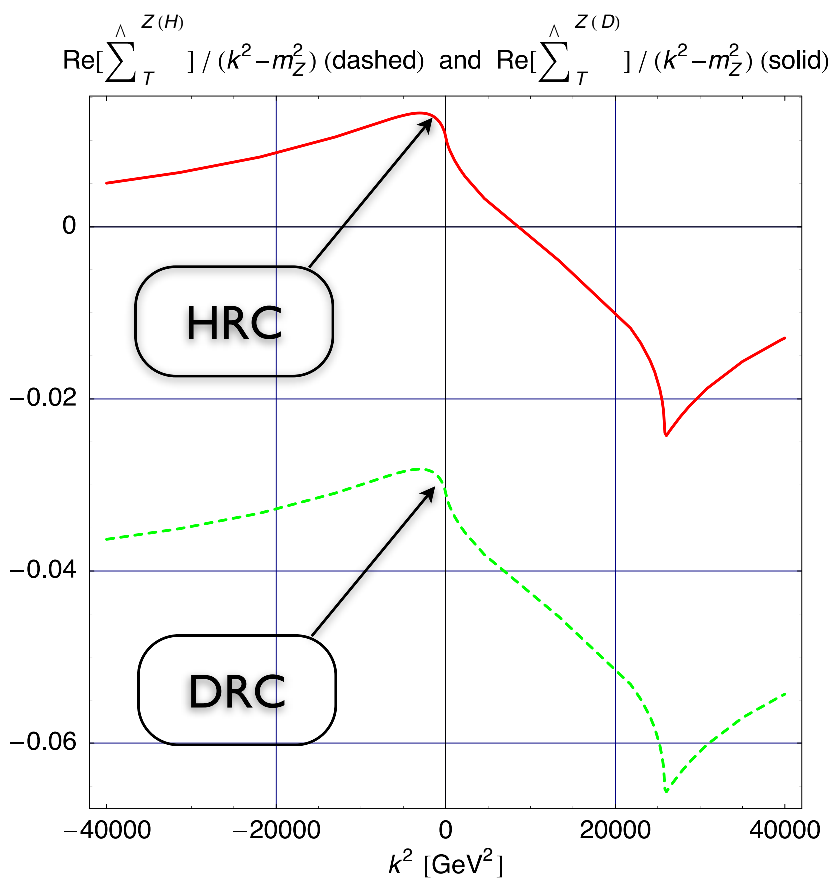

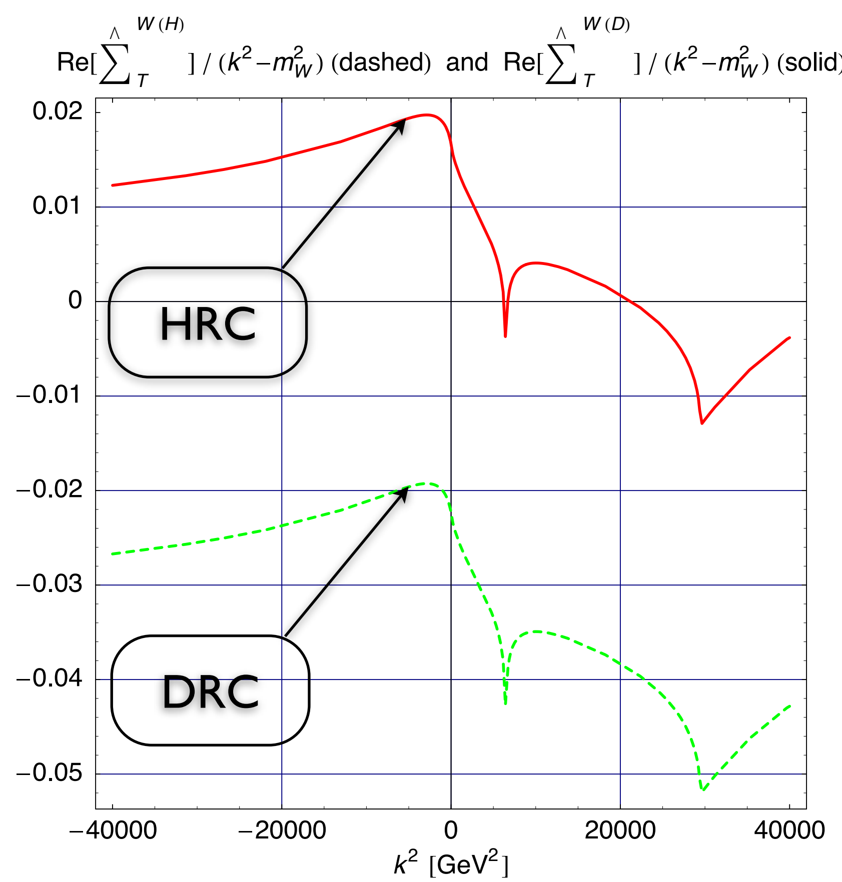

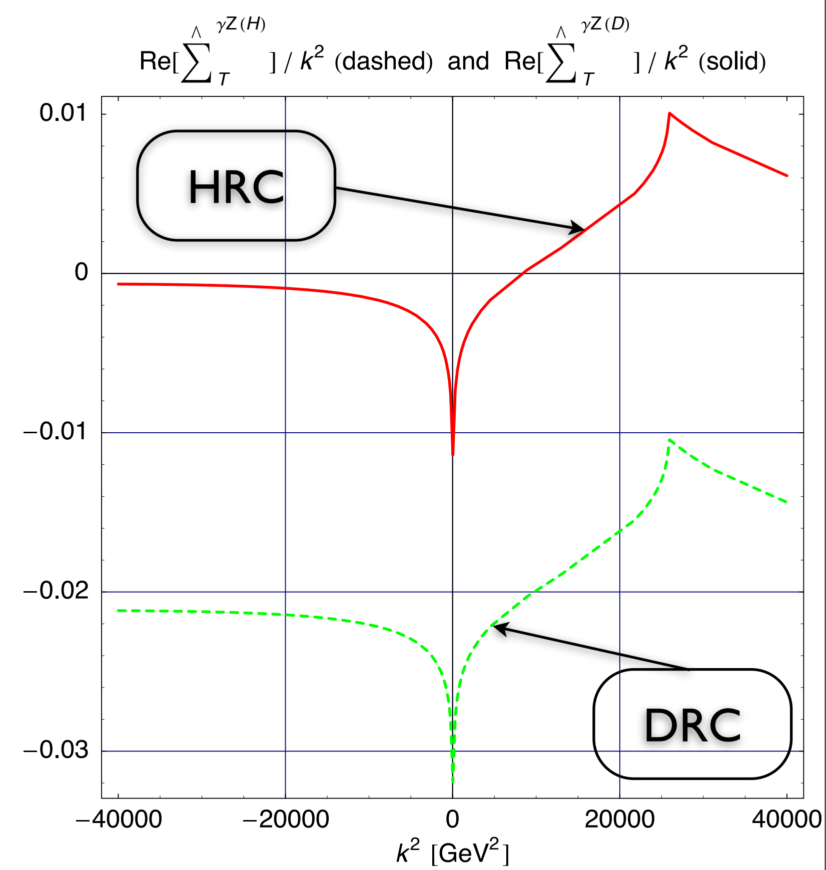

One-loop: photon emission

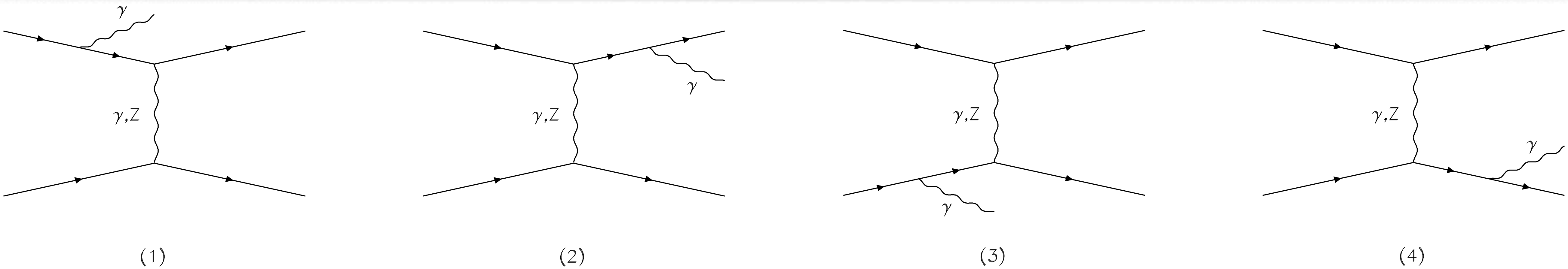

$$\sigma_{IR}^{Ver} + \sigma_{IR}^{\gamma\gamma-box} + \sigma_{IR}^{\gamma Z} = -\frac{2\alpha}{\pi} \log \frac{s}{\lambda^2} \log \frac{tu}{em^2 s} \sigma_0$$

$$\sigma^R = \sigma_{\text{IR}}^R + \sigma_H^R$$

$$\sigma_{IR}^R = \frac{2\alpha}{\pi} (\log \frac{4\omega^2}{\lambda^2} \log \frac{tu}{em^2 s} - \frac{1}{2} \log^2 \frac{s}{em^2} + \frac{1}{2} - \frac{\pi^2}{6} + \frac{1}{2} \log^2 \frac{u}{t}) \sigma_0$$

$$\sigma_H^R = \frac{2\alpha}{\pi} \log \frac{\Omega^2}{\omega^2} \log \frac{tu}{em^2 s} \sigma_0 + \sigma_H^{R,\Omega}$$

One-loop: results

The relative correction to the Born asymmetry A^0_{LR} is defined as follows:

$$\delta_A^C = \frac{A^C_{LR} - A^0_{LR}}{A^0_{LR}}$$

where index C means a specific contribution (C = BSE, Ver, Box, ...), A^0_{LR} is the Born asymmetry, and A^C_{LR} is the total asymmetry including electroweak radiative corrections.

Input parameters: α=1/137.035999,
m_W = 80.398 GeV,
m_Z = 91.1876 GeV.

$\sqrt{s}$, GeV	Result of Denner and Pozzorini	Our result
100	−0.2787	−0.2790
500	−0.3407	−0.3406
2000	−0.9056	−0.9066

Comparison of our result for the weak correction to asymmetry with the result of arXiv:hep-ph/9807446.

One-loop: results

The Born asymmetry A^0_{LR} and the structure of relative *weak* corrections to it for $E_{\rm lab} = 11$ GeV at different θ.

$\theta,^\circ$	20	30	40	50	60	70	80	90
A^0_{LR}, ppb	6.63	15.19	27.45	43.05	60.69	77.68	90.28	94.97
$\gamma\gamma$-SE, DRC	−0.0043	−0.0049	−0.0054	−0.0058	−0.0062	−0.0064	−0.0066	−0.0067
$\gamma\gamma$-SE, HRC	−0.0043	−0.0049	−0.0054	−0.0058	−0.0062	−0.0064	−0.0066	−0.0067
γZ-SE, DRC	−0.2919	−0.2916	−0.2914	−0.2912	−0.2911	−0.2910	−0.2909	−0.2909
γZ-SE, HRC	−0.6051	−0.6043	−0.6042	−0.6038	−0.6034	−0.6031	−0.6028	−0.6028
ZZ-SE, DRC	−0.0105	−0.0105	−0.0105	−0.0105	−0.0105	−0.0105	−0.0105	−0.0105
ZZ-SE, HRC	0.0309	0.0309	0.0309	0.0309	0.0309	0.0309	0.0309	0.0309
HV, DRC	−0.2946	−0.2633	−0.2727	−0.2703	−0.2714	−0.2712	−0.2711	−0.2710
HV, HRC	−0.0015	−0.0012	−0.0010	−0.0009	−0.0008	−0.0007	−0.0007	−0.0007
ZZ-box, exact	−0.0013	−0.0013	−0.0013	−0.0013	−0.0013	−0.0013	−0.0013	−0.0013
ZZ-box, approx.	−0.0013	−0.0013	−0.0013	−0.0013	−0.0013	−0.0013	−0.0013	−0.0013
WW-box, exact	0.0239	0.0238	0.0238	0.0239	0.0239	0.0238	0.0238	0.0238
WW-box, approx.	0.0238	0.0238	0.0238	0.0238	0.0238	0.0238	0.0238	0.0238
total *weak*, DRC, exact	−0.5643	−0.5430	−0.5508	−0.5489	−0.5500	−0.5495	−0.5493	−0.5493
total *weak*, HRC, approx.	−0.5526	−0.5514	−0.5511	−0.5505	−0.5500	−0.5496	−0.5493	−0.5493

One-loop: results and comparison

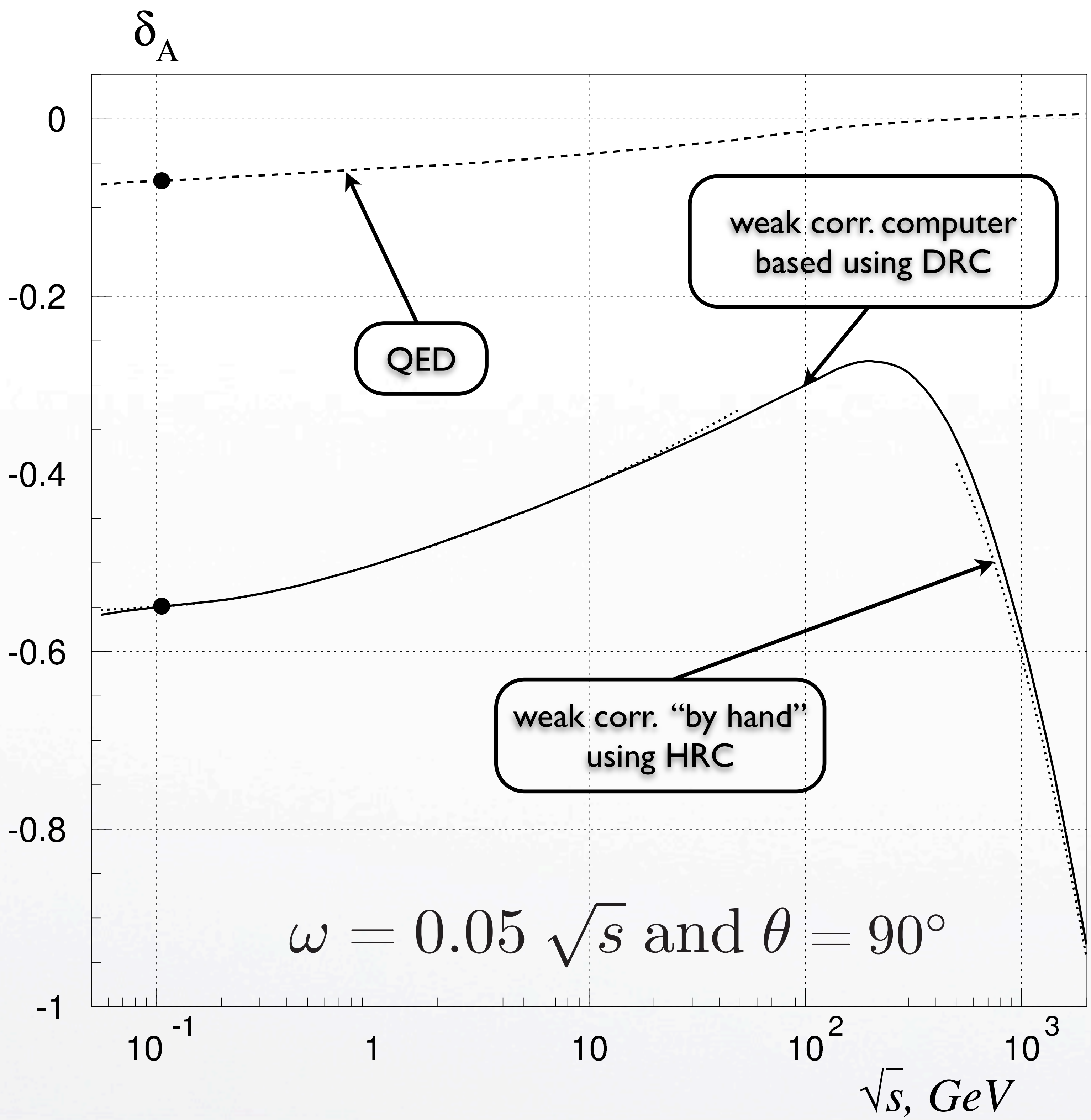

The relative weak (solid line in DRC (semi-automated) and dotted line in HRC ("by hand")) and QED (dashed line) corrections to the Born asymmetry A^0_{LR} versus $\sqrt{s}$ at $\theta = 90°$.

The filled circle corresponds to our predictions for the MOLLER experiment.

One-loop in different schemes: cross section

- Constrained Differential Renormalization (CDR): F. del Aguila et al., Phys. Lett. B 419 263 (1998)

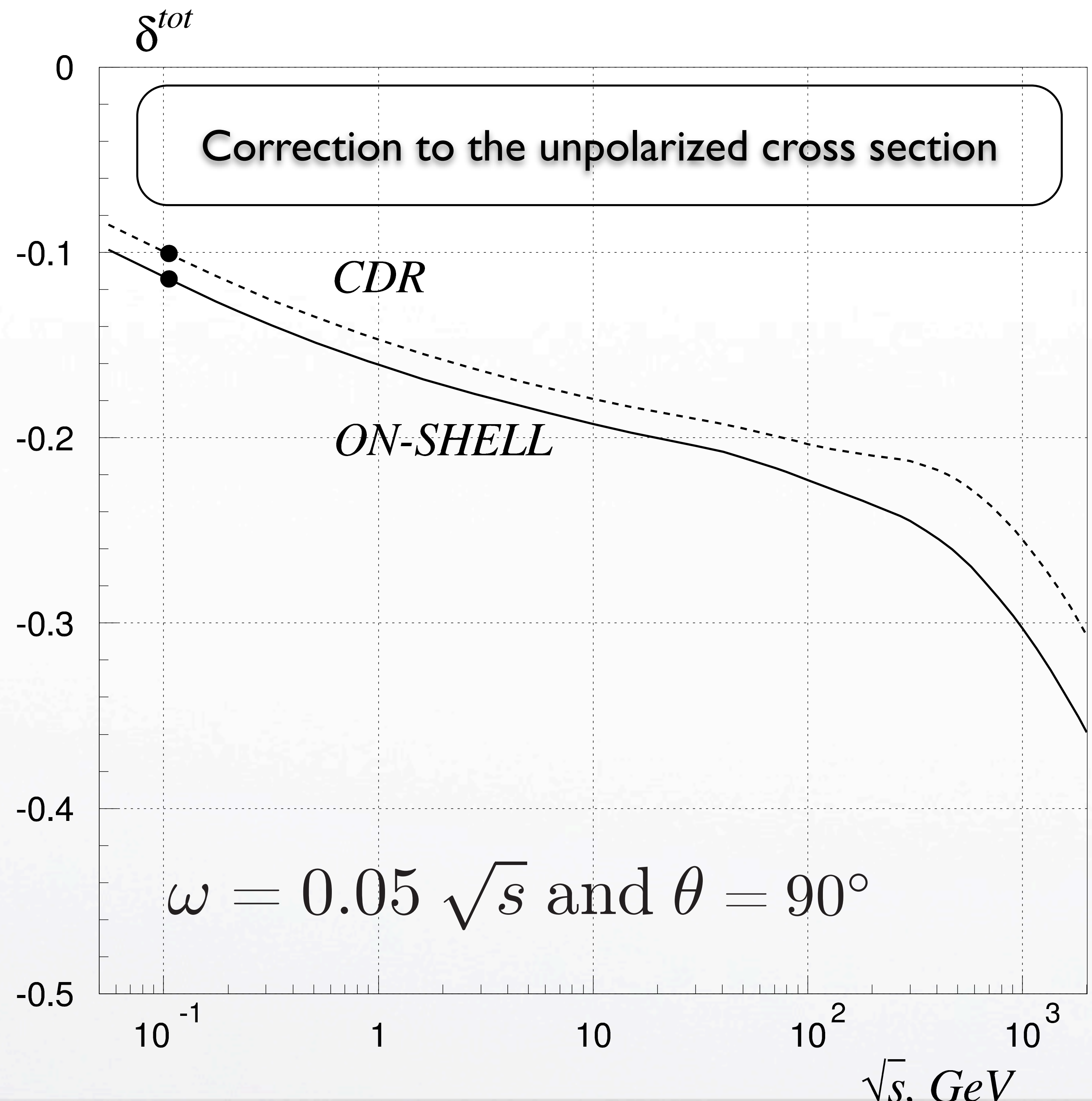

$$\delta^{\rm tot} = (\sigma^{\rm tot} - \sigma^0)/\sigma^0$$

In the region of small energies, the difference between the two schemes is almost constant and rather small (~ 0.01), but grows at $\sqrt{s} \geq m_Z$.

At small energies, the correction to the cross section is dominated by the QED contribution. However, in the high-energy region the weak correction becomes comparable to QED. Since the difference between the on-shell and CDR results grows substantially as the weak correction becomes larger, it is clear that for an observable such as the PV asymmetry the difference between the on-shell and CDR schemes will be sizeable for the entire spectrum of energies $\sqrt{s}$ < 2000 GeV.

One-loop in different schemes: asymmetry

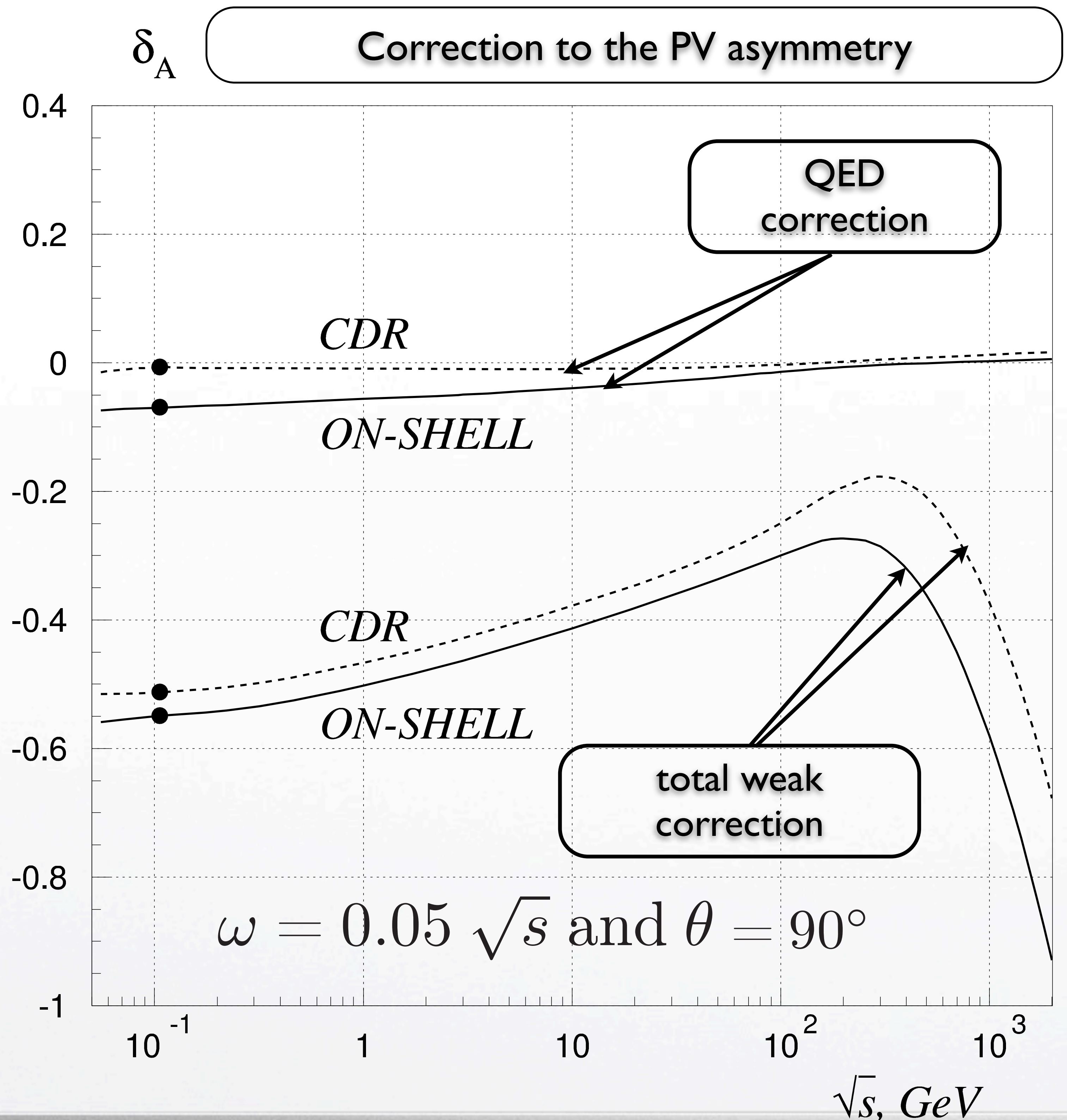

$$\delta_A^C = \frac{A_{LR}^C - A_{LR}^0}{A_{LR}^0}$$

- Correction to asymmetry differ in two schemes at the order of 10%.

- Higher order contributions are important!

The Next-to-Next-to-Leading Order (NNLP) EWC to the Born ($\sim M_0M_0^+$) cross section can be divided into two classes:

- Q-part induced by quadratic one-loop amplitudes $\sim M_1M_1^+$, and
- T-part – the interference of Born and two-loop diagrams $\sim 2\mathrm{Re}M_0M_{2\text{-loop}}^+$.

$$\sigma = \frac{\pi^3}{2s}|M_0 + M_1|^2 = \frac{\pi^3}{2s}(\underbrace{M_0M_0^+}_{\propto\,\alpha^2} + \underbrace{2\mathrm{Re}M_1M_0^+}_{\propto\,\alpha^3} + \boxed{\underbrace{M_1M_1^+}_{\propto\,\alpha^4})} = \sigma_0 + \sigma_1 + \boxed{\sigma_Q}$$

$$\sigma_T = \frac{\pi^3}{s}\,\mathrm{Re}M_2M_0^+ \propto \alpha^4$$

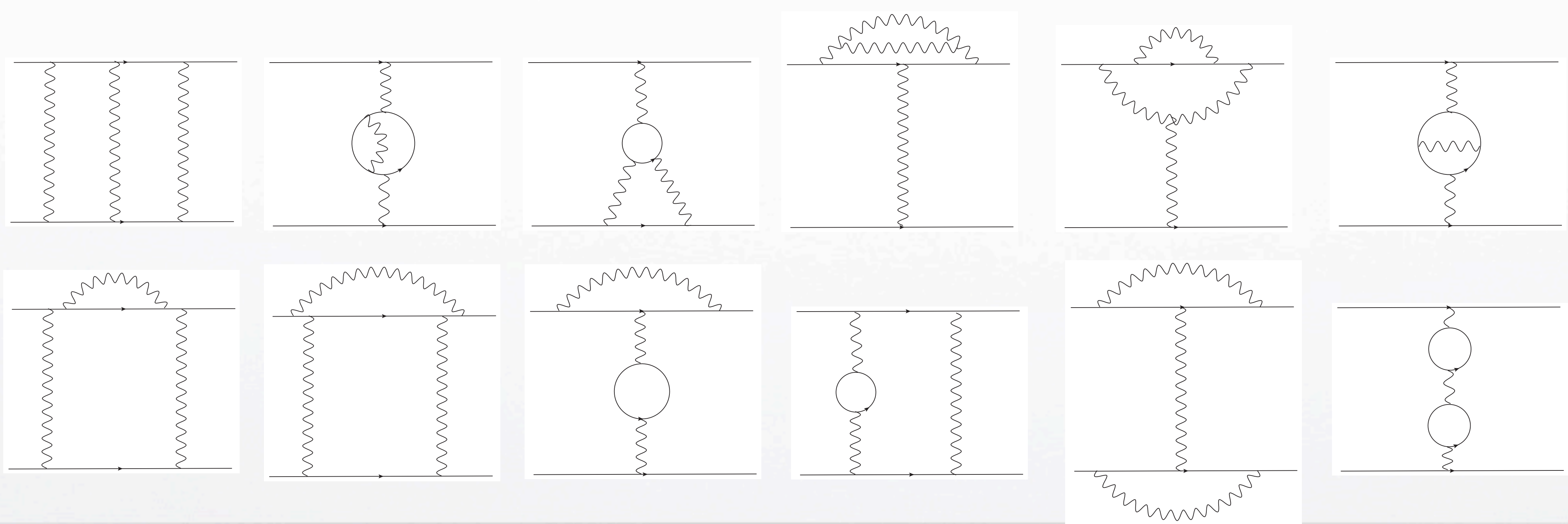

+ ...

Quadratic correction: IR part

Differential quadratic cross section σ_Q written as sums of λ-dependent (IRD-terms) and λ-independent (infrared-finite) parts.

$$\sigma_Q = \frac{\pi^3}{2s} M_1 M_1^+ = \underline{\sigma_Q^\lambda} + \underline{\sigma_Q^f}$$

$$\frac{\pi^3}{2s} M_1^{\lambda+}\left(M_1^\lambda + 2M_1^f\right) = \frac{1}{4}\left(\frac{\alpha}{\pi}\right)^2 \mathrm{Re}\left[\delta_1^{\lambda *}(\delta_1^\lambda + 2\delta_1^f)\right]\sigma_0 .$$

$$\left(\frac{\alpha}{\pi}\right)^2 \delta_Q^f\, \sigma_0$$

$$\delta_1^\lambda = 4B \log\frac{\lambda}{\sqrt{s}}$$

$$B = \log\frac{tu}{m^2 s} - 1 + i\pi$$

Quadratic correction: photon emission

In order to remove IR divergent terms in quadratic cross section it is required to consider:

1. Photon emission from one-loop diagrams
2. Two photon photon emission

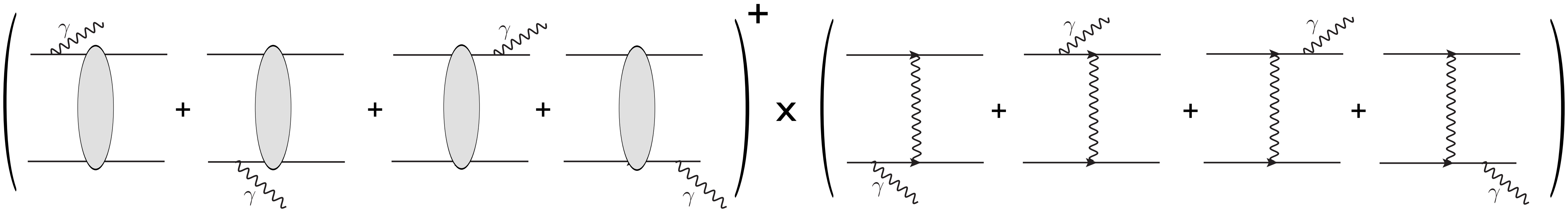

$$\sigma_Q^\gamma = \tfrac{1}{2}\sigma^\gamma = \frac{\pi^2}{s}\ \mathrm{Re}\left[(-\delta_1^\lambda + R_1)^* M_1^+ M_0\right]$$

$$R_1 = -4B\log\frac{\sqrt{s}}{2\omega} - \log^2\frac{s}{em^2} + 1 - \frac{\pi^2}{3} + \log^2\frac{u}{t}$$

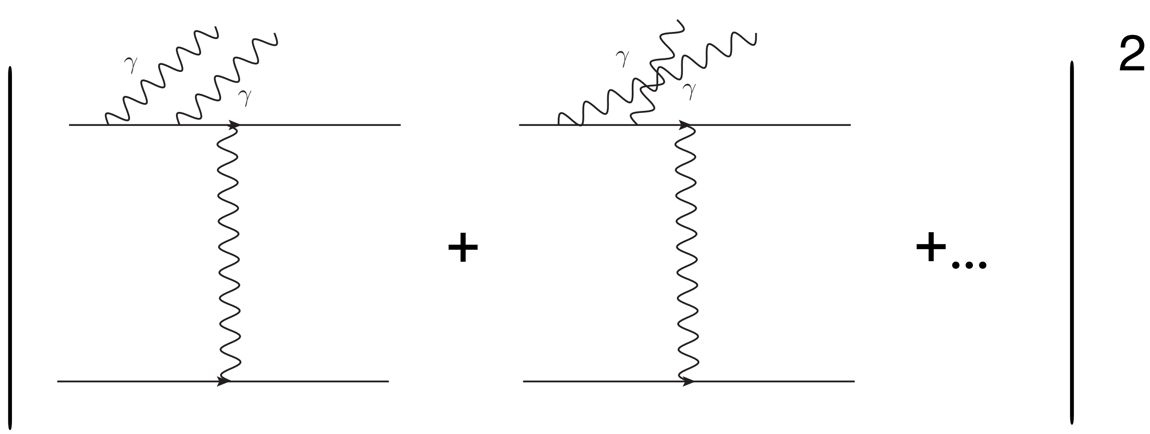

$$\sigma_Q^{\gamma\gamma} = \frac{1}{2}\sigma^{\gamma\gamma} = \frac{1}{4}\left(\frac{\alpha}{\pi}\right)^2\left(\left|-\delta_1^\lambda + R_1\right|^2 - R_2\right)\sigma_0$$

$$R_2 = \frac{8}{3}\pi^2(\log\frac{tu}{m^2 s} - 1)^2$$

Quadratic correction: photon emission

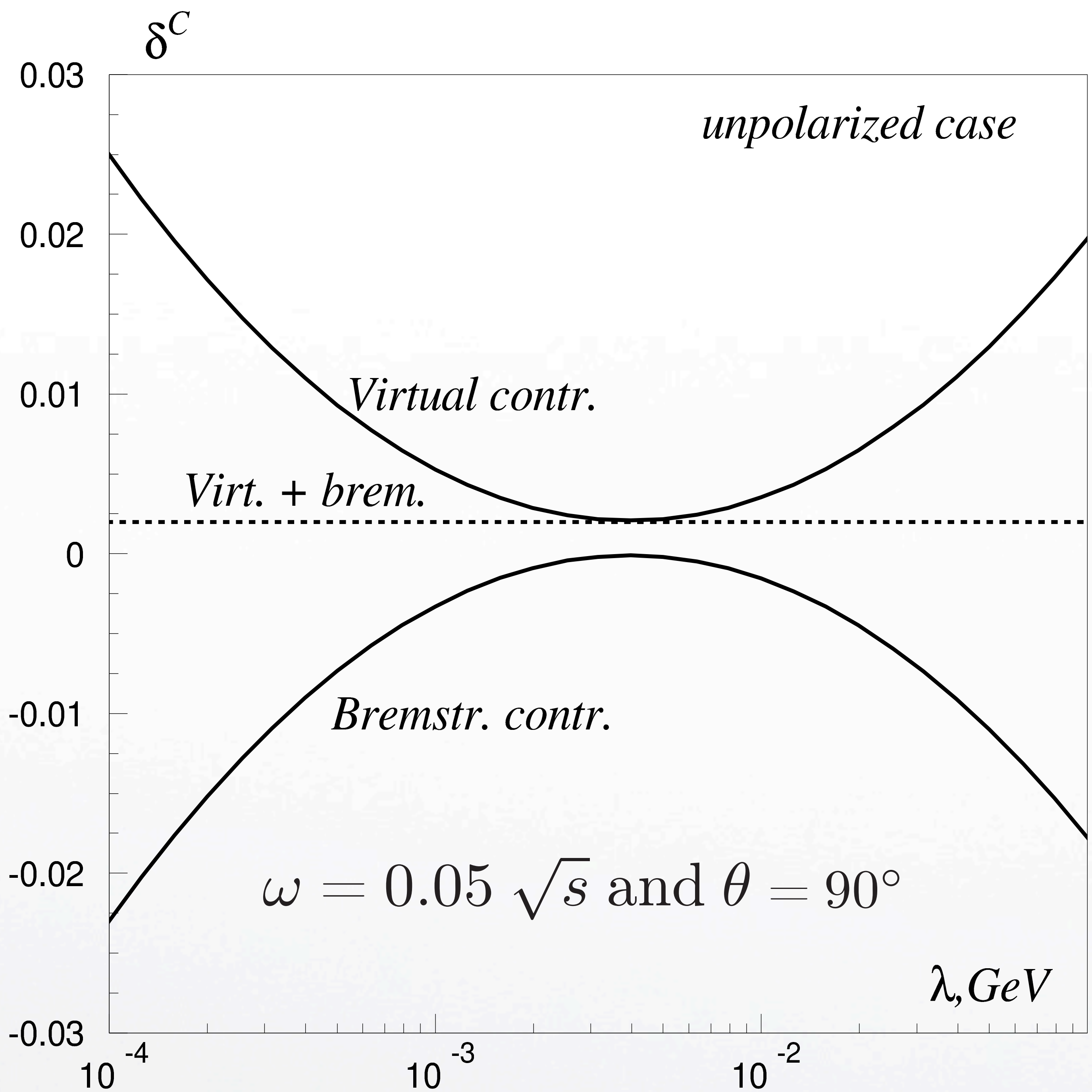

$$\delta^{\mathrm{C}} = (\sigma^{\mathrm{C}} - \sigma^{0})/\sigma^{0}$$

The plot for $\theta = 90^o$ and $E_{lab} = 11$ GeV, clearly demonstrates that the relative correction to unpolarized cross section is independent on the photon mass λ.

We can also see the quadratic dependence in log scale of λ for the both virtual and bremstrahlung contributions.

Quadratic correction: results

$$\delta_A^{\mathrm{C}} = (A_{LR}^{\mathrm{C}} - A_{LR}^{0})/A_{LR}^{0}$$

$$\Delta_A = (A_{LR}^{1-\mathrm{loop}+\mathrm{Q}} - A_{LR}^{1-\mathrm{loop}})/A_{LR}^{0}$$

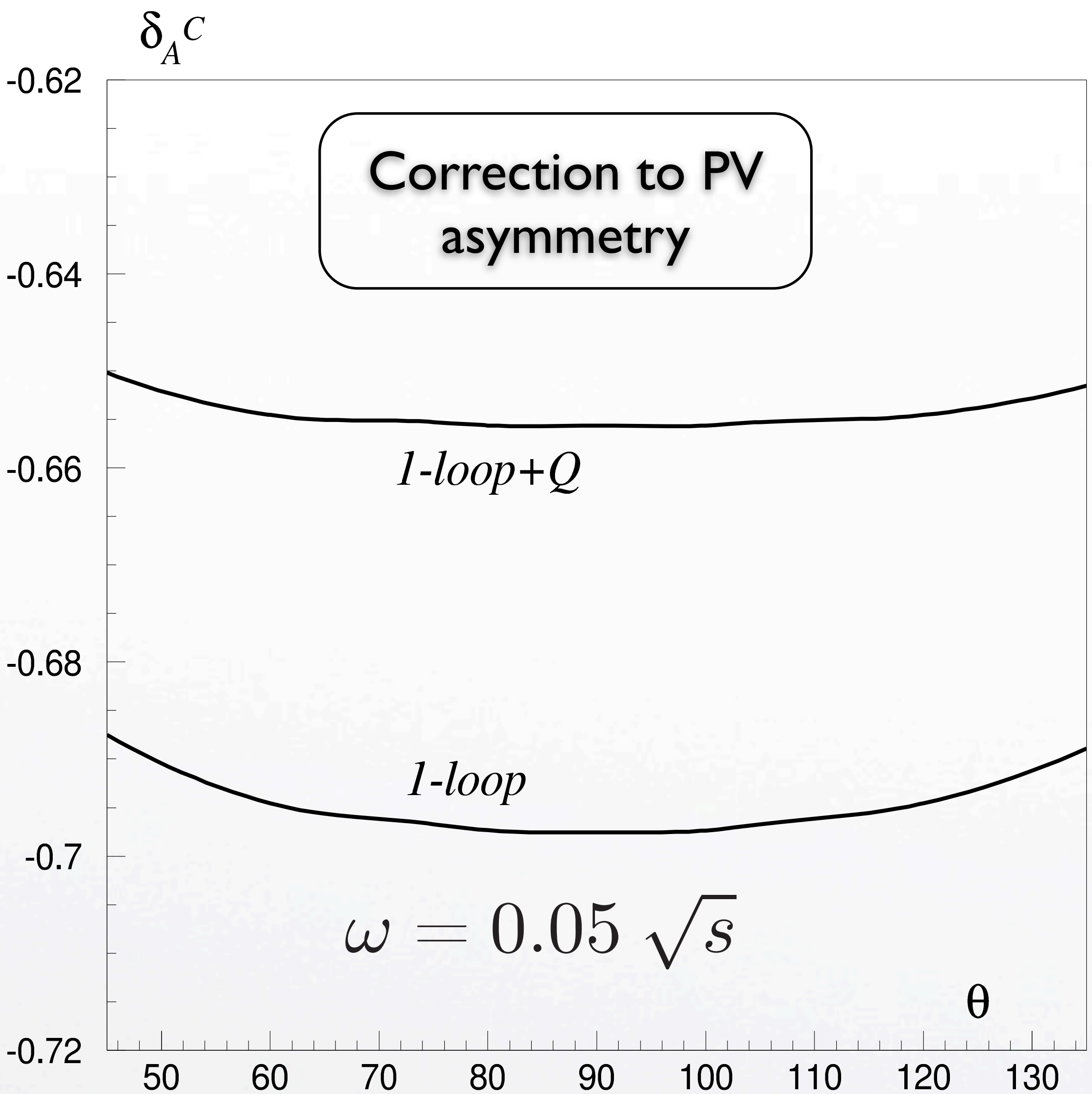

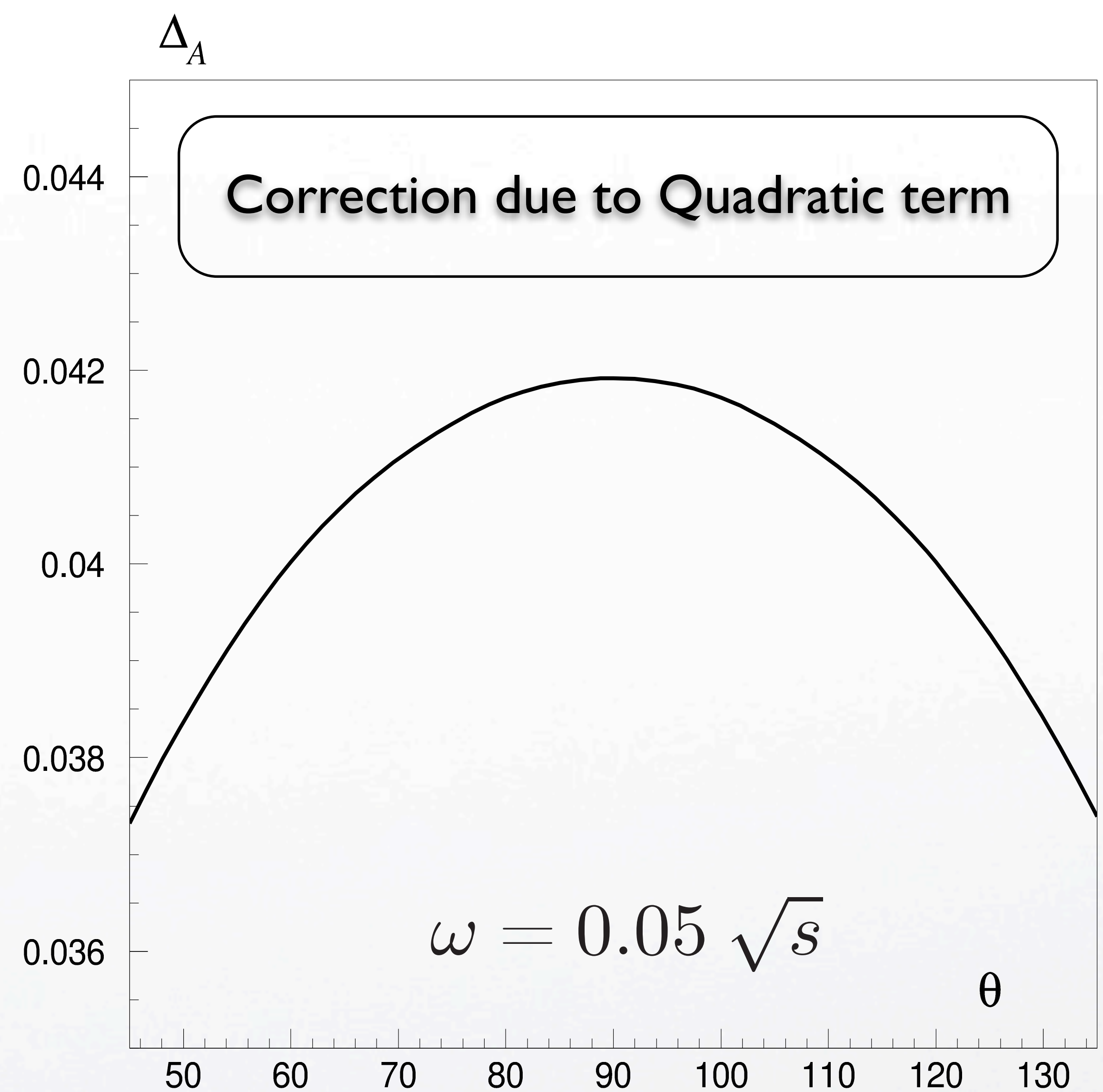

E_{lab} = 11 GeV

Quadratic correction: results

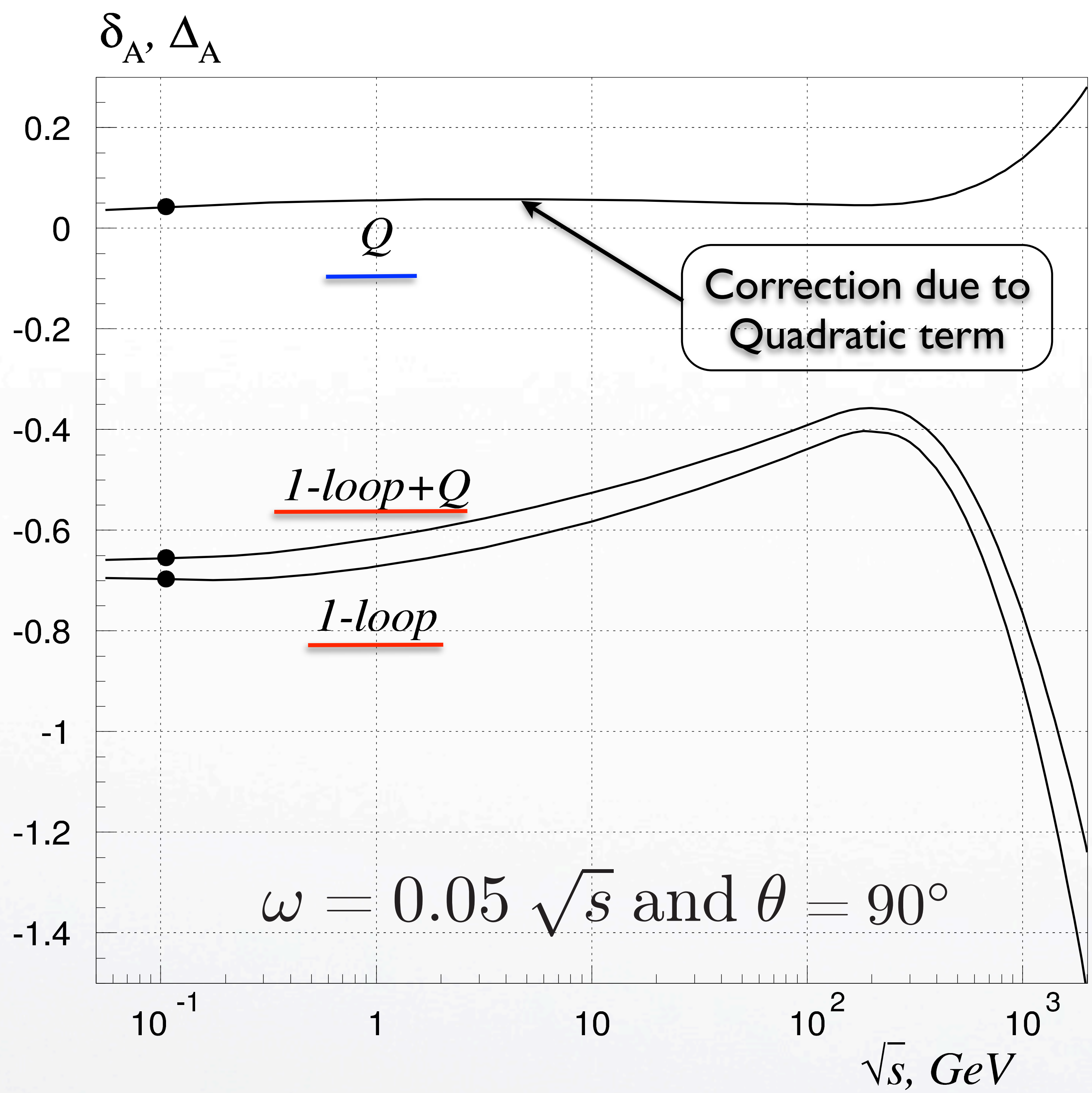

$$\delta_A^C = (A_{LR}^C - A_{LR}^0)/A_{LR}^0$$

$$\Delta_A = (A_{LR}^{1-\text{loop}+\text{Q}} - A_{LR}^{1-\text{loop}})/A_{LR}^0$$

The scale of the Q-part contribution in the low-energy region is approximately constant, but starting from $\sqrt{s} \geq m_Z$, where the weak contribution becomes comparable with electromagnetic, the effect of Q-part grows sharply.

This effect of increasing importance of two-loop contribution at higher energies may have a significant effect on the asymmetry measured at the future $e^- e^-$-colliders.

Conclusion

• EWC corrections depend quite significantly on the energy and scattering angles.

•At the MOLLER kinematic conditions, the part of the quadratic EWC we considered here can increase the asymmetry up to ~ 4%.

•For the high-energy region $\sqrt{s}$ ~ 2000 GeV the contribution of the quadratic EWC we estimated can reach +30%.

•The large size of the Q-part demands detailed and consistent consideration of two-loop corrections, which is the current task of our group. It is impossible to say at this time if the Q-part will be enhanced partially or completely cancelled by other two-loop radiative corrections, although it seems probable that the two-loop EWC may be larger than previously thought. Although an argument can be made that the two-loop corrections are suppressed by a factor of $\alpha\pi$ relative to the one-loop corrections, we are reluctant to dismiss them, especially in the light of 2% uncertainty to asymmetry promised by MOLLER.

•Excellent agreement we obtained between the results calculated "by hand" and semi automatically serves as a good illustration of opportunities offered by FeynArts, FormCalc, LoopTools, and FORM.